CONF-810701--6

THE DEVELOPMENT OF A MECHANISTICALLY BASED COMPUTER SIMULATION OF NITROGEN OXIDE ABSORPTION IN PACKED TOWERS*

R. M. Counce
Fuel Recycle Division
Consolidated Fuel Reprocessing Program
Oak Ridge National Laboratory
Oak Ridge, Tennessee 37830

ABSTRACT

A computer simulation for nitrogen oxide (NO_x) scrubbing in packed towers was developed for use in process design and process control. This simulation implements a mechanistically based mathematical model, which was formulated from (1) an exhaustive literature review, (2) previous NO_x scrubbing experience with sieve-plate towers, and (3) comparisons of sequential sets of experiments. Nitrogen oxide scrubbing is characterized by simultaneous absorption and desorption phenomena; the model development is based on experiments designed to feature these two phenomena. The model was then successfully tested in experiments designed to put it in jeopardy.

INTRODUCTION

The objective of this work is to build a fully predictive mechanistic model to describe the scrubbing of nitrogen oxides in packed towers. An evaluation of the literature and previous nitrogen oxide scrubbing experience in plate towers indicated that the key elements for such a model, the kinetic, equilibrium, and mass-transfer constants, were known or could be estimated at 298 K. Such a model is important because the scrubbing of nitrogen oxides involves several simultaneous absorption and desorption mechanisms, and the resultant complexity seems to rule out attempts at parameterization. Some mechanistic uncertainty remained after the initial formulation and required preliminary experimental information before tentatively entertaining a model. This model evolved further through a series of semi-structured sequential sets of experiments. A final set of experiments designed to jeopardize the model did not prove contradictory.

THEORETICAL BACKGROUND

The NO_x-HNO_x-H_2O chemical system can be described for engineering purposes by considering the important species to be NO, NO_2, N_2O_3, N_2O_4, HNO_x, and H_2O. The relative homogeneous and heterogeneous equilibrium proportions and the reactivity of these compounds in the gas and liquid phases form the theoretical basis for this study. This review first presents the important gas-phase reactions, then briefly contrasts the solubilities of the various NO_x species, and finally presents the important liquid-phase chemical reactions. The study of the liquid-phase chemical reactions first focuses on those reactions that contribute in a positive manner to the absorptive flux of NO_x species from the gas to the liquid phase. Attention will then be directed to the decomposition and/or depletion of aqueous HNO_2 produced by those previously mentioned reactions. This decomposition or depletion produces the desorptive flux of NO_x species associated with the scrubbing of NO_x species from gas streams.

Gas Phase Reactions. The following gas-phase reactions are of interest when describing the NO_x-HNO_x-H_2O systems (1):

$$2NO_2\,(g) \longleftrightarrow N_2O_4\,(g)\ , \tag{1}$$

$$NO\,(g) + NO_2\,(g) \longleftrightarrow N_2O_3\,(g)\ , \tag{2}$$

$$NO\,(g) + NO_2\,(g) + H_2O\,(g) \longleftrightarrow 2HNO_2\,(g)\ , \tag{3}$$

and

$$2NO\,(g) + O_2\,(g) \rightarrow 2NO_2\,(g)\ . \tag{4}$$

Usually, conditions that maximize the presence of gaseous N_2O_4, such as increased pressure and/or decreased temperature, will produce the maximum NO_x absorption for high gaseous NO_x partial pressures. Conditions that maximize the presence of gaseous N_2O_3 and/or HNO_2 provide maximum NO_x absorption efficiency for dilute gaseous NO_x partial pressures. To simplify the discussion of the several gaseous nitrogen oxide and oxiacid species, the terms "chemical" nitric oxide and nitrogen dioxide are used for +II and +IV valent nitrogen species as:

$$NO^* = NO + N_2O_3 + 1.2HNO_2\ , \tag{5}$$

and

$$NO_2^* = NO_2 + 2N_2O_4 + N_2O_3 + 1.2HNO_2 \tag{6}$$

Gas-Liquid Equilibria. The solubilities of NO_2^*-NO^* species range over several orders of magnitude (1). In order of increasing solubility, these species are listed as NO, NO_2, N_2O_3, N_2O_4, and HNO_2. The pressure of HNO_3 over dilute solution may be considered negligible. The importance of the solubilities of these species is somewhat overshadowed, however, by the fast hydrolytic reactions of N_2O_3 and N_2O_4 in the liquid phase.

Liquid Phase Reaction. In the liquid phase, the following reactions appear to be important to the absorption process:

$$2NO_2\,(l) + H_2O\,(l) \rightarrow HNO_3\,(l) + HNO_2\,(l)\ , \tag{7}$$

$$N_2O_4\,(l) + H_2O\,(l) \rightarrow HNO_3\,(l) + HNO_2\,(l)\ , \tag{8}$$

and

$$N_2O_3\,(l) + H_2O\,(l) \rightarrow 2HNO_2\,(l) \tag{9}$$

These reactions may be treated irreversibly at low aqueous concentrations of HNO_2 and HNO_3. The reaction of NO_2 and water is sufficiently slow to be considered as a bulk-phase reaction; thus, the absorption is related to the transfer of NO_2 into the bulk-liquid phase. The hydrolytic reactions of N_2O_4 and N_2O_3 are sufficiently fast to take place in the liquid film. The absorption rate for the ith species reacting in the liquid film by the film theory coupled with chemical reactions is (2)

$$R_i = (\sqrt{Dk})H_i P_i^*\ . \tag{10}$$

The absorption or combined absorption and reaction of gaseous NO_2^* or NO^* species result in the production of aqueous HNO_3 and/or HNO_2. Aqueous HNO_3 is relatively stable in this system, whereas aqueous HNO_2 is relatively unstable. The depletion chemistry of HNO_2 in aqueous solutions has been the subject of several investigations; however, the apparent combinations of mass transfer and chemical reaction have created a great deal of confusion in this area.

The best known equation for describing the depletion of aqueous HNO_2 from aqueous solutions is:

$$3HNO_2\,(l) \longleftrightarrow H^+\,(l) + NO_3^-\,(l) + H_2O\,(l) + 2NO\,(g)\ . \tag{11}$$

This overall equation was developed by Abel and Schmid (3, 4), who discovered the decomposition process to be fourth-order with respect to aqueous HNO_2:

$$r_{HNO_2} = -k_{11}\,\frac{C_{HNO_2}^4}{P_{NO}^2}\ . \tag{12}$$

Abel and Schmid (3, 4) recognized that the removal of NO from solution could limit the dissociation of aqueous HNO_2; therefore, these studies were conducted at conditions which reduced the mass-transfer resistances to the removal of NO from solution. Because of the equilibrium nature of the Abel-Schmid depletion process, as implied in Eq. (12), the rate controlling process can shift to the removal of NO from solution.

$$r_{HNO_2} = -(3/2)\,k_L a\,(C_{NO} - C_{NO}^*)\ . \tag{13}$$

*Research sponsored by the Nuclear Fuel Cycle Division, U.S. Department of Energy under Contract No. W-7405-eng-26 with Union Carbide Corporation.

under mass-transfer limiting conditions producing a reaction order of 4/3 with respect to HNO_2. So, other intermediate mixtures of mass transfer and chemical reaction can produce any reaction order between 4 and 4/3. The Abel-Schmid stoichiometry stipulates that the molar ratio of HNO_3 produced to HNO_2 decomposed to be 1/3. For convenience, this molar ratio is referred to as R*. This stoichiometry is in general agreement with that found by most researchers in HNO_2 depletion chemistry.

Some researchers [see review by Counce (11)], however, have found R* to be less than 1/3 in studies into the nonoxidizing depletion of aqueous HNO_2. The order (with respect to HNO_2) of the HNO_2 depletion reaction is usually equal to slightly greater than one for studies when R* is less than 1/3.

The decreasing value of R* suggests that species other than NO, such as HNO_2, can be desorbed during the depletion of HNO_2 from aqueous solutions. The first-order depletion kinetics and its sensitivity to gas rates and agitation further suggest that mass-transfer resistances are involved in this process. The aqueous HNO_2 depletion process might be represented, with respect to the indicated considerations, as

$$R_{HNO_2} = k_L a (C_{HNO_2} - C^*_{HNO_2}) = k_G a (P^*_{HNO_2} - P_{HNO_2}) \tag{14}$$

The stoichiometry of Eq. (14) produced an R* of zero. The value of R* for the nonoxidizing depletion of HNO_2 from aqueous solutions must then be between zero and 1/3.

Experimental Results on Depletion of Nitrous Acid from Aqueous Solutions. The depletion of nitrous acid from aqueous nitric-nitrous acid solutions during contact with nitrogen was investigated using columns packed with Intalox saddles as the contacting device. These studies were conducted at 298 K and near atmospheric pressure. The liquid phase was recirculated in these studies, which were designed to estimate the effects of gas flow rate, liquid flow rate, and column height on the depletion process(es).

The primary response variable was the conversion of aqueous nitrous acid in the packed tower. Another response variable was the molar ratio of HNO_3 produced to HNO_2 disappearing, R*; this parameter is an indicator of the extent that Eq. (11) describes the depletion process.

In experiments involving the contact of nitrous acid solutions with nitrogen, the hypothesis that R* is 1/3 was tested. The feed gas to the column during these operations contains no NO. In all runs, the feed and effluent liquid streams were sampled. These samples were analyzed for total acidity and nitrous acid. The total acidity was assumed to be the sum of the nitric acid and nitrous acids. Based on this assumption, the change in total acid concentration can be represented by

$$dC_{H^+} = dC_{HNO_3} + dC_{HNO_2} \tag{15}$$

The quantity, R*, can be obtained by rearranging Eq. (15),

$$R^* = \frac{dC_{HNO_3}}{dC_{HNO_2}} = 1 - \frac{dC_{H^+}}{dC_{HNO_2}} \tag{16}$$

In these studies, nitrous acid was produced initially by bubbling N_2O_3 through 0.025 m^3 of water in the liquid surge tank; nitric acid is produced simultaneously by some decomposition of HNO_2. This aqueous solution was then metered continuously to the packed column where it was contacted with nitrogen. The effluent solution from the column flowed by gravity back to the liquid surge tank. Recirculation of this solution provided a means of obtaining information on the depletion process(es) over a range of nitrous acid concentrations. The two packed towers used in these studies were 0.0762-m-ID with 6-mm Intalox saddles and 0.102-m-ID with 13-mm Intalox saddles.

The first series of experiments A through D utilized a fractional factorial design to study the effect of gas flow rate, liquid flow rate, and packing height (volume) on the extent of nitrous acid conversion, X_{HNO_2}, in the small diameter tower. The effects shown in Table 1 were estimated by Yates' algorithm (5). A main effect is the average change in response per unit change in process variable. The relative main effects, defined for component i by

$$\phi_i = \left(\frac{\text{main effect of } i \text{ on } X_{HNO_2}}{\text{average } X_{HNO_2}}\right)_{C_{HNO_2}} \tag{17}$$

is shown in Fig. 1.

Table 1. Experimental depletion conversion of HNO_2 for a fractional factorial study of the depletion of nitrous acid in packed towers

Variables	(Low)	(High)
L (volumetric liquid flow rate), $m^3 s^{-1}$	1.78 × 10^5	3.40 × 10^5
G (feed gas flow rate), $m^3 s^{-1}$	1.57 × 10^4	3.24 × 10^4
h (packing height), m	0.15	0.30

Variable arrangement				Removal efficiencies (X_{HNO_2}) at varied C_{HNO_2}				
				C_{HNO_2}				
Run	L	G	h	0.015	0.020	0.025	0.030	0.035
A		+		0.0038	0.0240	0.0449	0.0616	0.0750
B	+	+	+	0.0529	0.0676	0.0663	0.0692	0.0718
C			+	0.0657	0.0674	0.0703	0.0726	0.0746
D	+			0.0268	0.0340	0.0412	0.0487	0.0551
Average				0.0360	0.0470	0.0557	0.0629	0.0691
Effects of variables (Yates' method)								
			L	-0.0080	-0.0065	0.0039	0.0018	0.0017
			G	0.0018	0.0010	0.0007	0.0005	-0.0006
			h	-0.0049	-0.0014	-0.0075	-0.0016	-0.0018

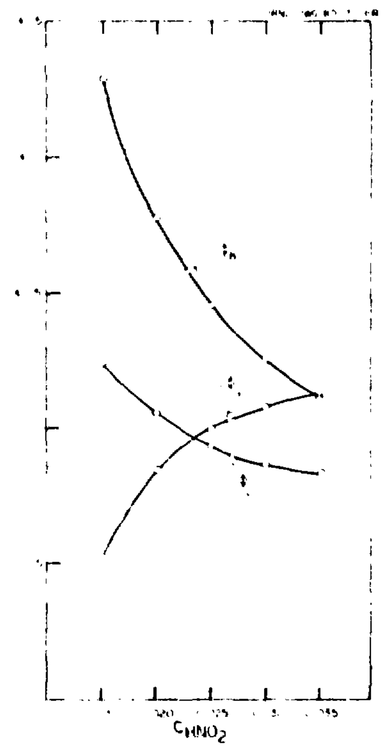

Fig. 1. The relative main effects of the manipulation of L, G, and h on X_{HNO_2} at varying C_{HNO_2}.

This analysis shows that as the concentration of nitrous acid entering the tower is increased, (1) the effect of the change in liquid flow rate decreases (actually shown to impede the depletion of nitrous acid at higher nitrous acid concentrations), (2) the effect of gas rate increases, and (3) the effects of the change in height generally decreases. The significance of these effects could not be determined because there is no measure of experimental error.

If it is assumed that mass-transfer is important to some extent in this depletion process, then it seems appropriate to view these experiments from a vantage point that includes how the indicated variable manipulation affects the mass-transfer resistances. The increased column height is directly proportional to interfacial area and liquid- and gas-residence time in the tower. The increase in liquid flow rate increases both the liquid-phase mass-transfer rate constant(s) and the gas-liquid interfacial area. The increase in gas flow rate increases the gas-phase mass-transfer rate constant(s). Based on the assumption of the importance of mass-transfer on the depletion of aqueous nitrous acid, the following

theory may be proposed for experiments A through D: (1) liquid-phase mass-transfer is becoming less important with increasing nitrous acid concentration, while the converse is true for the gas-phase mass-transfer, in other words, the primary mass-transfer resistance is shifting from the liquid to the gas-phase with increased nitrous acid concentration, and (2) the effect of additional interfacial area and residence times becomes of less importance with increasing nitrous acid strength. These indicated resistances must be combined with representative stoichiometric considerations to produce a useful model.

The quantity, R*, may be determined from the slope of C_H^* as a function of C_{HNO_2}, assuming that the liquid surge tank is well mixed. An example of these plots (for experiment A1) is presented in Fig. 2. The values of R* for experiments

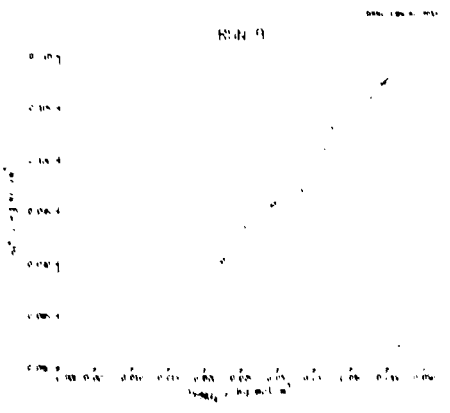

An example of the change in the system total acid concentration as a function of the changing concentration

gth D and the approximate 95% confidence intervals are presented in on this basis, the hypothesis that R* is 1/3 cannot be rejected.

Table 2. Values of R* and approximate 95% confidence intervals for experiments A through D

Run	R*	Degrees of freedom	Approximate 95% confidence interval for R*
A	0.22	4	(0.05, 0.39)
B	0.28	5	(0.18, 0.39)
C	0.30	6	(0.25, 0.35)
D	0.30	4	(0.21, 0.39)

Trends in the previously presented experiments indicating that R* decreased with the gas rate could not be verified. Another experiment was then conducted at much higher gas rate to liquid rate ratios. The value of R* was found to be 0.223 with a 95% confidence interval of 0.167 to 0.279. The order of these depletion processes was near one for most of the experiments presented.

The results from these experiments indicate that a mechanistic model for the depletion of aqueous nitrous acid in packed towers should include the liquid-phase decomposition as described in Eq. (11), followed by the desorption of nitric oxide, and the physical desorption of nitrous acid. The importance of simulating the gas- and liquid-phase resistances is also indicated.

MATHEMATICAL MODEL

The scheme that was tentatively entertained for describing mass-transfer and chemical-reaction phenomena for the NO_x-HNO_3-H_2O system is given in Fig. 3. This scheme is quite similar to one used previously by Hoftyzer and Kwanten (6), who illustrated conceivable transfer and reaction routes involved in NO_x scrubbing. The present model, as diagramed in Fig. 3, allows for calculations in the bulk-gas phase, within the liquid film, and the bulk-liquid phase. The gas phase is assumed to be saturated with H_2O (taking into consideration the temperature and the liquid HNO_3 concentration). The indicated gaseous chemical equilibria were assumed to apply at all times in the gas phase. The predicted HNO_3 partial pressure is usually small compared with the H_2O partial pressure and is always assumed to be equal to or below the saturation partial pressure. The model accommodates the oxidation of gaseous NO to NO_2 in the bulk-gas phase.

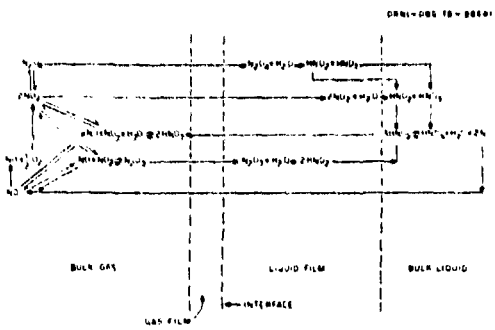

Fig. 3. Model for describing mass-transfer and chemical-reaction phenomena.

The steady-state transport of component i across both the gas and liquid films is expressed by Counce (1) as:

$$R_i = k_{G,i} \frac{dP_i}{d\xi} = (1 k_L)_i (C_i^* - C_i) \quad (11a)$$

utilizing a dimensionless film thickness.

In the case of physical absorption or desorption, the enhancement factor I is taken to be unity. The absorbing species as NO_2, N_2O_4, and N_2O_3. From the work of Carriveau (7), Denbigh and Prince (8), Koval and Peters (9), and Peters and Koval (10), it may be concluded that HNO_2 is not an absorbing species although it cannot be ruled out as a desorbing species. The other desorbing species is NO, which is formed from the bulk-liquid-phase decomposition of HNO_2.

COMPUTER SIMULATION

The absorption/desorption phenomena involved in the scrubbing of nitrogen oxides from gas streams have been simulated in a computer code for an incremental column volume, which is illustrated in Fig. 4. The volume of this incremental

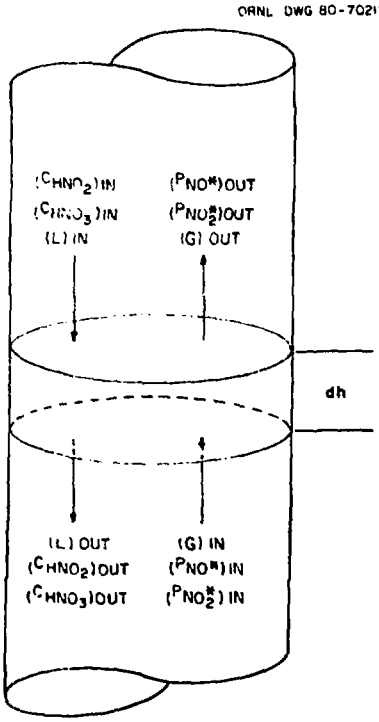

Fig. 4. Representation of incremental volume in a packed tower.

section is such that the change in component partial pressures and concentrations, as well as gas and liquid flow rates in the increment, may be neglected in rate equations for interphase transport. The gas phase is assumed to be ideal, and isothermal conditions are further assumed to prevail. The mathematical model shown here is designed to be used in the computation of the partial pressures of gas species leaving the increment and concentrations of liquid species entering the increment, and is based on known or assumed information about the gas and liquid streams respectively entering and leaving the same increment. The mode of operation for this study consists of beginning the computation at the bottom of the column with experimentally observed information about the gas-phase composition and flow rate and the liquid flow rate; the liquid-phase acid compositions are initially estimated at this point from experimental observations. The program advances up the tower by a series of incremental calculations. When the computation reaches the top of the tower, the calculated concentrations of acid are compared to the experimentally observed values (usually zero, as water was normally used as the scrub solution). If these values are greater than preset limits, the computation is begun again at the bottom of the tower with adjusted product acid concentrations. This procedure is repeated until the calculated values of the feed acid concentrations are sufficiently close to the experimentally observed values. At this point, the overall NO_x conversion X_{NO_x} is calculated, the results are printed as output, and the program operation is terminated.

A flowsheet of the computer simulation is shown in Fig. 5. The simulation consists of a main program and a collection of subroutines, all in FORTRAN.

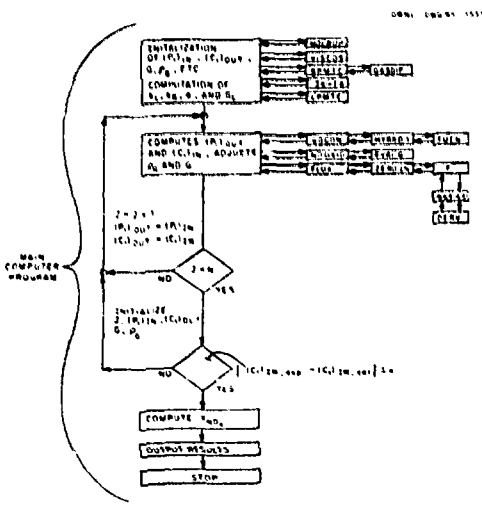

Fig. 5. Flowsheet of computer simulation.

The first portion of the main program initializes the temperature, pressure, and gas flow rate into the tower and liquid flow rate from the tower; the component partial pressures of oxygen, nitrogen, and nitrogen oxides are also initialized. In addition, NO^+ and NO_2^+ are also initialized, and the liquid-phase acid concentrations are estimated. The main program then sequentially calls subroutines for standard gas- and liquid-phase transport quantities associated with packed towers.

The liquid-phase holdup is calculated in subroutine HOLDUP. This calculation is based on an equation by Kwanten and Huiskamp (11). The gas-phase mass-transfer coefficients are calculated using an equation by Onda et al. (12) in GPMTC; this calculation requires the gaseous diffusivities in GASDIF using an equation by Fuller, Schettler, and Giddings (13). The gas-liquid interfacial area is calculated in IAREA using an equation by Puranik and Vogelpohl (14). The liquid-phase coefficients are calculated in LPMTC using an equation by Mohunta et al. (15).

Equations (1), (2), and (3) are incorporated in the sum and difference of Eqs. (5) and (6) as

$$P_{NO_T} + P_{NO_2} + P_{NO_2} + 2K_1 P_{O_2}^{1/2} + 2K_2 P_{NO} P_{NO_2} + (K_1 P_{H_2O} P_{NO} P_{NO_2})^{1/2} \quad (19)$$

and

$$0 = P_{NO_2} + 2K_1 P_{O_2}^{1/2} - P_{NO} \quad (20)$$

These equations contain two unknowns, P_{NO} and P_{NO_2}, and are contained in a subroutine function FUCN. The two previous equations are solved numerically using the HYBRD1 subroutine (16).

The conversion of nitric oxide to nitrogen dioxide is calculated using subroutine NOOXID; this is currently a bisection routine which finds the root X_{NO} (1) of

$$\frac{k_L a P_{NO}^* (P_{O_2})_{in} V}{G_T} - \frac{1}{1+b}\left[\frac{1}{1-X_{NO}} - \frac{b}{1+b}\ln\frac{1+b\,X_{NO}}{1-X_{NO}}\right] = 0 \quad (21)$$

The previous equation is contained in a subroutine EVALG.

The individual flux equations for the individual NO_x species may be expressed in terms of NO and NO_2 with appropriate equilibrium constants. The change in the partial pressure across a dimensionless film thickness, ξ, is (1)

$$\frac{dP_{NO_2}}{d\xi} = \frac{\alpha_8 (R_{NO_2^+}) + \alpha_9 (R_{NO^+})}{\alpha_{10}\alpha_8 - \alpha_{11}\alpha_{12}} \quad (22)$$

This equation for P_{NO}^* has been solved numerically by a "shooting" method using subroutines RKF45 and ZEROIN (17), which are called from the subroutine FLUX. This solution requires the evaluation of

$$P_{NO} = \frac{\alpha_7 P_{NO_2} + \alpha_2 (P_{NO_2})^2 - \alpha_{12} P_{NO_2}}{2\alpha_{10}} - \frac{\alpha_9 P_{NO_2}^* + \alpha_7 P_{NO}^* + \alpha_3 C_{NO}}{2\alpha_{10}} \quad (23)$$

at each integration step. Equations (22) and (23) are contained in the subroutine function F.

The absorption of HNO_2 is not allowable by the previously presented mathematical model. In order to prevent the absorption of HNO_2, the single component flux of HNO_2 is tested; if the flux is absorptive then $k_L HNO_2$ is made equal to zero. This will allow the desorption of HNO_2 and prevent its absorption.

With the calculation of P_{NO}^* and $P_{NO_2}^*$, the individual partial pressure flux components may be calculated in FLUX.

The partial pressures of NO_2^+ and NO^+ leaving the increment are calculated in the MAIN program as

$$(P_{NO_2^+})_{out} = (P_{NO_2^+})_{in} - (R_{NO_2^+} + 2R_{N_2O_4} + R_{N_2O_3} + 1.28R_{HNO_2})(\Delta V R T / G_T) + P_{NO}^* X_{NO} \quad (24)$$

and

$$(P_{NO^+})_{out} = (P_{NO^+})_{in} - (P_{N_2O_3} + 1.28R_{HNO_2} + R_{NO^+})(\Delta V R T / G_T) - P_{NO}^* X_{NO} \quad (25)$$

in terms of total nitrogen oxide partial pressure.

$$(P_{NO_x})_{out} = (P_{NO_x})_{in} + (P_{NO})_{out} \quad (26)$$

Further adjustments of the gas flow rate and component partial pressures due to bulk-gas component removal or addition are made before beginning the next incremental calculation.

Focusing on the liquid phase of the incremental column volume, the absorption reactions produce aqueous nitric and nitrous acids. The equilibrium as expressed in Eq. (11), is assumed to apply. This equilibrium reaction proceeds to the right as NO desorbs from the aqueous phase. The absorption of NO is neglected because of its low solubility. The bulk-phase concentration of NO is calculated from a modified Abel-Schmid equilibrium expression (3, 4).

$$C_{NO} = \left(\frac{a_{HNO_2}^3}{H_{NO}^2 K_{aa} a_{H^+} a_{NO_3^-}}\right)^{1/2} \quad (27)$$

Thus, the production of nitric acid in the increment because of decomposition may be represented by $\frac{1}{3}k_{LNO}(C_{NO} - C_{NO}^*)$ and the disappearance of nitrous acid by $3/2k_{LNO}(C_{NO} - C_{NO}^*)$. Incorporating these relationships into the liquid-phase performance equation and rearrangement yields:

$$(C_{HNO_3})_o = (C_{HNO_3})_{in} + (1/2 R_{NO_2} + R_{N_2O_4} - 1/2 R_{NO})(a\Delta V/L) , \quad (28)$$

and

$$(C_{HNO_2})_o = (C_{HNO_2})_{in} + (1/2 R_{NO_2} + R_{N_2O_4} + 2R_{N_2O_3} + R_{HNO_2} + 1/2 R_{NO})(a\Delta V/L) \quad (29)$$

By knowing or assuming $(P_{NO_2^*})_{in}$, $(P_{NO^*})_{in}$, $(C_{HNO_2})_{in}$, and $(C_{HNO_3})_{in}$, similar quantities may be calculated at the top of the increment provided R_i, in the liquid phase, may be calculated for the individual NO_x species.

Some further adjustment of the volumetric gas flow rates and component partial pressures is necessitated in the described computations because of the removal of gaseous species in bulk quantities. These adjustments are accomplished between the described incremental computations.

EXPERIMENTAL APPARATUS AND PROCEDURE

Two packed columns were used with inside diameters of 0.076 and 0.102 m respectively. These columns were packed with ceramic Intalox saddles with diameters of 6 and 13 mm respectively.

In the 0.076-m-diam column, the gas was entered into the packing through the packing support; however, the gas was rejected directly into the bottom of the packing in the 0.102-m-diam column. Both feed and effluent liquid streams were manually sampled.

Carrier gases of air or N_2 were metered by rotameter to either of the two packed towers. NO_2^* or NO^*-NO_2^* feed mixtures were produced by blending in the correct portions of these gases. Steam could also be added to this feed gas. The gas stream leaving the packed tower was cooled and demisted for entrained acid recovery and for control of the water content.

The gas analysis for NO^*-NO_2^* was done by taking gas samples for standard wet chemical analysis or by passing a gas stream through infrared detectors for NO^* and NO_2^* analyses. Liquid samples were also taken for nitrous and total acid analysis.

RESULTS

A screening series of tests was initially conducted to get a broad understanding of NO_x absorption in packed towers. The response variable is the NO_x conversion X_{NO_x}. This series of tests is presented in Table 3. At a 95% level of confidence, the only significant effects are the partial pressure and the oxidation state of NO_x in the feed gas. The most pronounced effect on the NO_x conversion was produced by variation in the oxidation state of the gas. This is a well-known phenomenon in NO_x scrubbing. In general, the NO^* species have a much lower overall solubility and reactivity than the NO_2^* species. The second largest effect was produced by the variation in the partial pressure of NO_x in the feed gas. This might be explained by the higher NO_x partial pressure producing a larger proportional amount of the higher molecular weight species, which are more absorbable and reactive.

Table 3. Data for fractional factorial design for studying seven NO_x scrubbing variables in eight runs

Variables	(Low)	(High)
Superficial liquid flow (m³/m²·s)	5.0 × 10⁻⁴?	5.25 × 10⁻³?
[illegible] HNO₃ [illegible]	0	3.0?
Partial pressure of NO_x [illegible]	0.005?	0.20
[illegible]	0	5.0 × 10⁻⁴?
[illegible] gas	Nitrogen	Air
[illegible] liquid temperature (K)	286?	300
Oxidation state of NO_x in feed gas	0.5?	1.0

Run	1	2	3	4	5	6	7	Overall NO_x conversion X_{NO_x}
A					•			69?
B	•			•			•	86?
C		•		•	•	•	•	91?
D	•	•				•		72?
E			•			•	•	90?
F	•		•	•	•	•		78?
G		•	•	•				82?
H	•	•	•		•		•	96?
Effect [illegible]	4.9?	0.6?	11.8?	7.6?	6.4?	5.6?	20.6?	

The parameters affecting X_{NO_x} that a design engineer has at his/her disposal are superficial liquid and gas velocity, column height, temperature, and pressure. The operating pressure was maintained at near atmosphere primarily for convenience. The 298 K operating temperature was chosen because the kinetic and equilibrium constants necessary for the model computation are fully defined only at this temperature. The experimental strategy was to model the effects of gas rate, liquid rate, and column height on the conversion of X_{NO_x} at moderate NO_x partial pressures of NO_2^* and then to test this model at low NO_x partial pressures with a feed mixture of NO_2^*/NO^*.

The bulk of these scrubber model development studies dealt with manipulations of gas rate, liquid rate, and column height. These studies are illustrated in Fig. 6. The originally planned experiments were a fractional factorial design (see solid outline in Fig. 6). Several experiments were sequentially added to examine the curvature of the response with column height. Other experiments were deleted after little effect of liquid rate was noted in the originally planned and probing experiments.

ORNL–DWG 81–1332

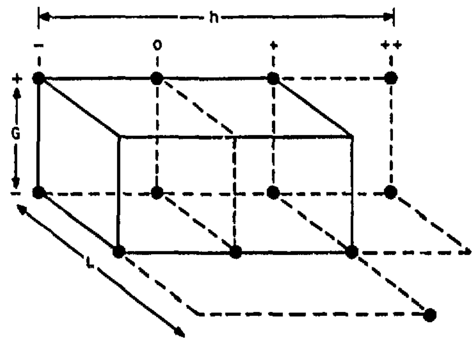

Fig. 6. Diagram showing planned and conducted experiments for parameter study of column height, gas rate, and liquid flow rate. The original factorial design is shown as dark-lined cube

The only adjustable coefficient in the model was $(\sqrt{Dk}/H)_{N_2O_4}$. Several experimenters have published values of this constant ranging from 5.7×10^{-4} to 11×10^{-4} kmol · atm⁻¹ · m⁻² · s⁻¹ (7, 18). The value of $(\sqrt{Dk}/H)_{N_2O_3}$, obtained by Corriveau (7), is the only such constant known. The effect of the ionic strength on these constants should be minimal since these studies were conducted using a water/dilute-acid scrub solution. The values of K_1, K_2, and K_3 were obtained from the works of Verhoek and Daniels (19), Beattie and Bell (20), and Wayne and Yost (21), respectively. The use of these constants maintained consistency as they have been used in the calculations of $(\sqrt{Dk}/H)_{N_2O_4}$ and $(\sqrt{Dk}/H)_{N_2O_3}$. The Henry's Law constants for NO, NO_2, and HNO_2 were from the International Critical Tables by Loomis (22), Lee and Schwartz (23), and Abel and Neusser (24), respectively. The rate constant for the oxidation of NO had little effect in these studies. The coefficient used in these calculations was that of Bodenstein (25). The value of K_{11} was from the work of Abel and Schmid (4).

The most critical coefficient is the value of $(\sqrt{Dk}/H)_{N_2O_4}$. Model computations using the literature values of this coefficient were tested to see which most accurately represented the data. The absorption of N_2O_4 was calculated to represent nearly all the NO_2^* absorption in the previously presented data. Model predictions of X_{NO_x} using the literature value of $(\sqrt{Dk}/H)_{N_2O_4}$ from Dekker et al. (18) allowed the model predictions to most accurately represent the data. An indication of this is seen in Fig. 7.

Results from a series of experiments with a 5% NO_x feed of partially oxidized feed gas were reasonably well simulated by the model being tested; however, the basic calculated absorption route was N_2O_4 absorption. The model was apparently not jeopardized in these tests.

A series of tests at feed NO_x partial pressures at ~0.01 atm is presented in Table 4. A considerable range of values of X_{NO_x} was encountered in these tests. The predominant absorption routes apparently shifts from N_2O_4 absorption for the highly oxidized feed gas to NO_2-N_2O_3 absorption for the less oxidized feeds. The model was deemed to be sufficiently jeopardized in these tests and this phase of model development was concluded.

CONCLUSION

The development of the model presented here gives a greater insight into the phenomena of nitrogen oxide scrubbing. The use of this mechanistically based mathematical model presented gives greater confidence in extrapolative situations such as process design. This model is not yet in a convenient form for use in design tasks. A recent example of such a design code is the ABNOX

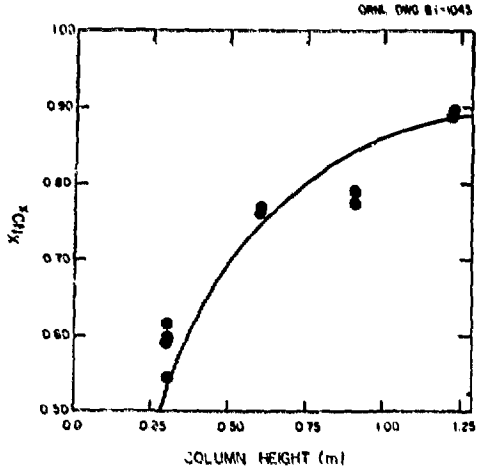

Fig. 7. The model-predicted and experimental conversion of NO_x obtained at varying heights of packing in the 0.10-m-diam tower; other parameters were $G = 3.2 \times 10^{-3}$ m$^3 \cdot$s^{-1}, $L = 3.8 \times 10^{-4}$ m$^3 \cdot$s^{-1}, $Y_{NO_x,in} = 0.03$ and $P_T = 1.1$ atm.

Table 4. Experimental and calculated results for runs with the NO_x feed partial pressure at almost 0.01 atm

Variable	Value	Weight
Gas rate (m$^3 \cdot$s^{-1})	3.4×10^{-3}	3.4×10^{-3}
Liquid rate (m$^3 \cdot$s^{-1})	3.8×10^{-4}	3.8×10^{-4}
Percent of NO_x with N_2O_3 feed	50	100

Run	Variable 0	2	3	$(X_{NO_x})_{exp}$	$(X_{NO_x})_{cal}$
30-32-21		•	•	0.64	0.62
30-32-26				0.80	0.82
30-32-20	•	•		0.80	0.86
30-32-28	•		•	0.85	0.84

[a] Calculated X_{NO_x} is based on $\sqrt{Dk}/H_{N_2O_4}$ of 1.0×10^{-5}

PROGRAM, which incorporates experimental and theoretical information on NO_x scrubbing in plate type towers in a convenient form for process design usage (26).

ACKNOWLEDGMENTS

This work was performed in the Fuel Recycle Division under the auspices of the Consolidated Fuel Reprocessing Program of the Oak Ridge National Laboratory and was sponsored by the Nuclear Fuel Cycle Division, U.S. Department of Energy, under Contract W-7405-eng-26 with Union Carbide Corporation.

NOTATION

a	gas-liquid interfacial area (m^{-1})
a_i	activity of *ith* species (kmol $\cdot$ m^{-3})
b	$P_{NO}/2P_{O_2}$
C_i	bulk-liquid concentration of component *i* (kmol $\cdot$ m^{-3})
C_i^*	interfacial concentration of component *i* (kmol $\cdot$ m^{-3})
d	differential operator
D	diffusivity (m$^2 \cdot$s^{-1})
E_i	enhancement factor, the factor by which the absorption of component i is increased by liquid reaction
(g)	gas
G	volumetric gas flow rate (m$^3 \cdot$s^{-1})
h	height of packing
H	Henry's law constant (m^3 atm $\cdot$ kmol^{-1})
HNO_x	$HNO_2 + HNO_3$
in	in
k	a first-order or a pseudo-first-order rate constant (s^{-1})
k_4	a third-order reaction rate constant for the oxidation of gaseous NO
k_{11}	a fourth-order reaction rate constant for the decomposition of gaseous HNO_2
K_1	an equilibrium constant defined by $P_{N_2O_4}/P^2_{NO_2}$ (atm^{-1})
K_2	an equilibrium constant defined by $P_{N_2O_3}/P_{NO}P_{NO_2}$ (atm^{-1})
K_3	an equilibrium constant defined by $P^2_{HNO_2}/P_{NO}P^2_{NO_2}P_{H_2O}$ (atm^{-1})
K_{11}	an equilibrium constant defined by $C_H + C_{NO_3} \rightleftharpoons C^2_{NO}/C^2_{HNO_2}$ (kmol $\cdot$ m^{-3})
k_G	gas-phase mass-transfer coefficient (kmol $\cdot$ m$^{-2} \cdot$ atm$^{-1} \cdot$ s^{-1})
$k_{G,i}$	gas-phase mass-transfer coefficient for component i (kmol $\cdot$ m$^{-2} \cdot$ atm$^{-1} \cdot$ s^{-1})
k_L	liquid-phase mass-transfer coefficient (m $\cdot$ s^{-1})
$k_{L,i}$	liquid-phase mass-transfer coefficient for component *i* (cm $\cdot$ s^{-1})
ln	base e logarithmic function
L	liquid flow rate (m$^3 \cdot$ s^{-1})
(l)	liquid
NO*	$NO + N_2O_4 + 1/2HNO_2$
NO_x^*	$NO_2 + 2N_2O_4 + N_2O_3 + 1/2HNO_2$
NO_x	$NO^* + NO_2^*$
out	out
P_i	bulk-gas partial pressure of component i or partial pressure of component i at ξ_k in the intermediate region encountered in numerical integration between $\xi = 0$ and $\xi = 1$ where $\Delta\xi$ is defined as $\xi_{k+1} - \xi_k$ (atm)
P_i^*	interfacial partial pressure of component i or partial pressure of component i at ξ_{k+1} in the intermediate region encountered in numerical integration between $\xi = 0$ and $\xi = 1$ where $\Delta\xi$ is defined as $\xi_{k+1} - \xi_k$ (atm)
P_T	total pressure (atm)
r_i	reaction rate for component i (kmol $\cdot$ m$^{-3} \cdot$ s^{-1} or atm $\cdot$ s^{-1})
R	gas law constant (m$^3 \cdot$ atm $\cdot$ kmol$^{-1} \cdot$ K^{-1})
R*	molar ratio of HNO_3 produced to HNO_2 disappearing
R_i	absorption rate for component i (kmol $\cdot$ m$^{-2} \cdot$ s^{-1})
V	column volume (m^3)
X_i	fractional conversion of component i; that is, $X_{NO_x} = 1(P_{NO_x})_{in} - (P_{NO_x})_{out}]/[(P_{NO_x})_{in} + \epsilon(P_{NO_x})_{out}]$
Y_i	mole fraction of component i
α_1	$k_{G,NO_2} + (k_L/H)_{NO_2}$
α_2	$2k_{G,N_2O_4}K_1 + 2(\sqrt{Dk}/H)_{N_2O_4}K_1$
α_3	k_{G,NO_2}
α_4	$2k_{G,N_2O_4}K_1$
α_5	$k_{G,NO}$
α_6	$k_{L,NO}$
α_7	$K_{L,NO}/H_{NO}$
α_8	$k_{G,N_2O_3}K_2P_{NO_2} + \frac{1}{4}k_{G,HNO_2}(K_3P_{H_2O}P_{NO_2}/P_{NO})^{1/2} + k_{G,NO}$
α_9	$k_{G,N_2O_3}K_2P_{NO_2} + \frac{1}{4}k_{G,HNO_2}(K_3P_{H_2O}P_{NO}/P_{NO_2})^{1/2}$
α_{10}	$k_{G,NO_2} + 4k_{G,N_2O_4}K_1P_{NO_2} + k_{G,N_2O_3}K_2P_{NO} + \frac{1}{4}k_{G,HNO_2}(K_3P_{H_2O}P_{NO}/P_{NO_2})^{1/2}$
α_{11}	$k_{G,N_2O_3}P_{NO_2} + \frac{1}{4}k_{G,HNO_2}(K_3P_{H_2O}P_{NO_2}/P_{NO})^{1/2}$
α_{12}	$k_{G,N_2O_3}K_2P_{NO} + \frac{1}{4}k_{G,HNO_2}(K_3P_{H_2O}P_{NO}/P_{NO_2})^{1/2}$
ΔV	incremental column volume (m^3)
Δ	signifies a difference in the final and initial values
ξ	dimensionless film thickness
ρ_G	density of gas (kmol $\cdot$ m^{-3})
ρ_L	density of liquid (kmol $\cdot$ m^{-3})
ψ_i	stoichiometric factor
ξ	$P_{NO_x}^* - P_{NO}^*$
ϵ	fractional volumetric change due to bulk removal of gas components

LITERATURE CITED

1. Counce, R. M., *The Scrubbing of Gaseous Nitrogen Oxides in Packed Towers*, Ph.D. Dissertation, The University of Tennessee, Knoxville (1980).

2. Danckwerts, P. V., *Gas Liquid Reactions*, Chapter 9, McGraw-Hill, New York (1970).

3. Abel, E. and H. Schmid, "Kinetics of Nitrous Acid III, Kinetics of the Decomposition of Nitrous Acid," *Z. Phys. Chem.* **134**, 279, translated from German (ORNL-tr-4264) (1928).

4. Abel, E. and H. Schmid, "Kinetics of Nitrous Acid IV, Equilibrium of Nitrous Acid-Nitric Oxide Reaction in Connection with its Kinetics," *Z. Phys. Chem.* **136**, 430, translated from German (ORNL-tr-4265) (1929).

5. Box, G. E. P., W. G. Hunter, and J. S. Hunter, *Statistics for Experimenters*, Wiley, New York (1978).

6. Hoftyzer, P. J. and F. J. G. Kwanten, *Processes for Air Pollution Control*, 2nd ed., Chapter 5B, Chemical Rubber Company, Cleveland (1972).

7. Cornwell, C. D., Jr., "The Absorption of N_2O_3 into Water," Master's thesis, University of California, Berkeley (1971).

8. Denbigh, K. G. and A. J. Prince, *J. Chem. Soc.* **59**, 316 (1947).

9. Koval, E. J. and M. S. Peters, "Reactions of Aqueous Nitrogen Dioxide," *Ind. Eng. Chem.* **52**, 1011 (1960).

10. Peters, M. S. and E. J. Koval, "Nitrogen Oxide Absorption in an Agitated Reactor," *Ind. Eng. Chem.* **51**, 577 (1959).

11. Kwanten, F. J. G. and J. Huskamp, *Processes for Air Pollution Control*, 2nd ed., Chapter 5A, Chemical Rubber Company, Cleveland (1972).

12. Onda, K. H. Takeuchi and Y. Okumoto, "Mass Transfer Coefficients Between Gas and Liquid Phases in Packed Tower," *J. Chem. Eng. J.* **1**, 56 (1969).

13. Fuller, E. N., P. D. Schettler, and J. C. Giddings, "A New Method for Prediction of Binary Gas-Phase Diffusion Coefficients," *Ind. Eng. Chem.* **58** (5), 18 (1966).

14. Putanik, S. S. and A. Vogelpohl, "Effective Interfacial Areas in Irrigated Packed Columns," *Chem. Eng. Sci.* **29**, 501 (1974).

15. Mohunta, D. M., A. S. Vaidyanathan, and G. S. Laddha, "Predictions of Liquid-Phase Mass-Transfer Coefficients in Columns Packed with Raschig Rings," *Indian Chem. Eng.* **11** (3), 73 (1969).

16. More, J. J., B. S. Garbow, and K. E. Hillstrom, *User's Guide for MinPack-1*, ANL-80-74 (1980).

17. Forsythe, G. E., M. A. Malcolm, and C. B. Moler, *Computer Methods for Mathematical Computations*, Prentice-Hall, Englewood Cliffs, N. J. (1977).

18. Dekker, W. A., E. Snoeck, and H. Kramers, "The Rate of Absorption of NO_2 in Water," *Chem. Eng. Sci.* **11**, 61 (1959).

19. Verhoek, F. H. and F. J. Daniels, "The Dissociation of Nitrogen Tetroxide and of Nitrogen Trioxide," *J. Am. Chem. Soc.* **53**, 1250 (1931).

20. Beattie, J. R. and S. W. Bell, "Dinitrogen Trioxide, Part I. Stability in the Gaseous Phase," *J. Chem. Soc.* **79**, 1681 (1957).

21. Wayne, F. G. and D. M. Yost, "Kinetics of the Rapid Gas Phase Reaction Between NO, NO_2, and H_2O," *J. Chem. Phys.* **19**, 41 (1961).

22. Loomis, A. L., *International Critical Tables III*, 255, McGraw-Hill, New York (1928).

23. Lee, Y. N. and S. E. Schwartz, "Reaction Kinetics of Nitrogen Oxides with Liquid Water at Low Partial Pressures," paper submitted to *J. Phys. Chem.* (1980).

24. Abel, E. and E. Neusser, "The Vapor Pressure of Nitrous Acid," *Monatsh. Chem.* **54**, 855, translated from German (OLS-79-369) (1929).

25. Bodenstein, M., "Velocity of Reaction Between Nitric Oxide and Oxygen," *Z. Elektrochem.* **24**, 183, translated from German (71-21320) (1918).

26. Counce, R. M., *A User's Guide to ABNOX, A Computer Program Designed to Simulate the Nitrogen Oxide Removal Efficiency of a Multistage Bubble-Cap Tower*, ORNL/TM-6938 (September 1979).